Environmental Challenges 3 (2021) 100043

Contents lists available at ScienceDirect

Environmental Challenges

journal homepage: www.elsevier.com/locate/envc

Fabrication of thin film sensors by spin coating using sol-gel $LaCrO_3$ Perovskite material modified with transition metals for sensing environmental pollutants, greenhouse gases and relative humidity

Prashant Bhimrao Koli, M.Sc. (Chemistry), SET[a,*], Kailas Haribhau Kapadnis, M.Sc. (Chemistry), Ph.D.[b], Uday Gangadhar Deshpande, M.Sc. (Chemistry), Ph.D.[c], Umesh Jagannath Tupe, M.Sc. (Electronics), SET[d], Sachin Girdhar Shinde, M.Sc. (Chemistry), SET, NET, GATE[e], Raju Shivaji Ingale, M.Sc. (Physics), SET[f]

[a] *Research Centre in Chemistry, Arts, Commerce and Science College, Nandgaon, Taluka-Nandgaon-423106, District-Nashik. Affiliated to SPPU, Pune, Maharashtra, India*

[b] *Research Centre in Chemistry and PG Department of Chemistry, Loknete Vyankatrao Hiray Arts, Science and Commerce College, Panchavati, Nashik-422003, Affiliated to SPPU,Pune, Maharashtra, India*

[c] *Research Centre in Chemistry and PG Department of Chemistry, Pratap College of Arts, Science and Commerce, Amalner, Taluka-Amalner-425401, District-Jalgaon. Affiliated to KBC-NMU Jalgaon, Maharashtra, India*

[d] *Research Centre in Electronics and PG Department of Electronics, Loknete Vyankatrao Hiray Arts, Science and Commerce College,Panchavati, Nashik-422003. Affiliated to SPPU, Pune Maharashtra, India*

[e] *Research Centre in Chemistry, Krantiveer Vasantrao Naik Arts, Science and Commerce College, Canada Corner, near Gangapur road, Nashik-422005. Affiliated to SPPU, Pune, Maharashtra, India*

[f] *Department of Physics, MITWPU School of Polytechnic and Skill Development, Shivtirthnagar, kothrud, Pune-411038. Affiliated to AICTE, Mumbai, Maharashtra, India*

ARTICLE INFO

Keywords:
Modified $LaCrO_3$ sensor
Greenhouse gas sensor
BET
TEM
Relative humidity

ABSTRACT

In this study, we are reporting the fabrications of undoped $LaCrO_3$ and Ni^{2+}, Fe^{3+}, Co^{2+} modified $LaCrO_3$ thin films by spin coating method using the sol-gels prepared for these thin film samples. The structural properties of the spin coated $LaCrO_3$ thin films measured by X-ray diffractometer (XRD), which confirms the formation of orthorhombic $LaCrO_3$ nanoparticles. The morphological properties of the prepared films were investigated by the ease of scanning electron microscopy (SEM), and high-resolution transmission electron microscopy (HR-TEM) where the orthorhombic and crystalline $LaCrO_3$ nanoparticles were observed. Energy dispersive x-ray analysis (EDAX) was utilized for the determination of elemental composition. The prepared material was found be in perfect elemental composition. The surface area and BJH pore distribution was observed by Brunauer-Emmett-Teller (BET) analysis. The Ni^{2+}, Fe^{3+}, Co^{2+} modified $LaCrO_3$ thin film found with high surface area of 86.32 m^2/g. Optical properties of both prepared materials investigated by ultraviolet differential reflectance spectroscopy (UV-DRS) to compare band gap energy of prepared sensors. It is observed that due to modification of transition metals, band gap energy of modified $LaCrO_3$ sensor is found to be declined. The electrical properties were carried out to confirm semiconducting behaviour of $LaCrO_3$ semiconductor. The thin films were subjected for gas sensing study of CO, CO_2, NO_2, LPG, toluene vapours and petrol vapours. The modified $LaCrO_3$ sensor found to be highly sensitive for CO_2, CO, and NO_2 gases with response 82.14 (300 °C), 74.52 (200 °C) and 65.18% (150 °C) respectively. The relative humidity from 10 to 90% at 20 Hz found to be efficient for modified $LaCrO_3$ sensor. In summary it can stated that transition metal doping successful to tune the band gap energy, porosity and surface area of modified $LaCrO_3$ sensor. Due to this the sensor properties such as% response,% selectivity, response recovery, reusability and humidity sensing performance found to enhance for modified $LaCrO_3$ sensor.

1. Introduction

The nanoparticles are very efficient materials which are extensively utilized by large number of researchers and scientist for their inherent applications. The solid materials are classified into various categories. One of the various classes of materials is Perovskite oxide materials where two metals are in identical oxidation like +III or two metals

* Corresponding author.
E-mail addresses: prashantkoli005@gmail.com (P.B. Koli), drugdeshpande@gmail.com (U.G. Deshpande), sachings@gmail.com (S.G. Shinde).

https://doi.org/10.1016/j.envc.2021.100043
Received 30 November 2020; Received in revised form 5 February 2021; Accepted 5 February 2021

with different oxidation state such as II, IV, in combination with three oxygen. In most of the literature the Perovskite materials referred as ABO_3 type solid material (Tan et al., 2014; Slonopas et al., 2019). The first Perovskite material synthesis according to reports was $CaTiO_3$. After that large number of Perovskite material were synthesized and used by the researchers for various catalytical applications (Chen et al., al.,2013; Jain et al., al.,2006; Ding and Xue, 2010; Huang et al., 2014; Zhang et al., al.,2020). There are many facile methods for the fabrication of Perovskite oxides such as very popular sol-gel, co-precipitation, micro fluids, hot injections, cation/anion exchange, combustion, chemical vapour deposition, electrochemical methods, spray Pyrolysis, magnetic sputtering, ball milling, solid state reaction etc. (Morozova et al., 2017; Zhang et al., 2014; Koli et al., 2020).

These Perovskite metal oxides and similar materials, commonly employed in various applications such as solar cells, electrochemical applications, light emitting diodes, sintering, drug delivery, biochemical process, glass and optical lenses, Lasers, piezoelectric sensors, electroluminescence, surface chemistry, SOFC, optoelectronics, thin/thick film sensors, photo detectors and another catalytic application (Adeel et al., 2020; Bataglioli et al., 2019; Koli et al., 2019; Jiao et al., 2020; Kim et al., 2016; Koli et al.2018; Shinde et al., 2020; Koli et al., al.,2018). The purpose behind the use of these materials results from their high thermal stabilities, excellent sensitivities, energy storage abilities, simple synthesis, high accessibilities and selectivity, natural inherent catalytic properties, etc. The Perovskite materials reported for electronic application in commercialized form are listed as Metal halide Perovskite like $CsPbX_3$ (X=Cl, Br, I), $CsNiBr_3$, metal oxide Perovskite like $LaFeO_3$, $LaCrO_3$ etc. (Zhang et al., al.,2016).

The undoped $LaCrO_3$ is utilized in huge numbers of the applications as reported previously. The undoped LaCrO3 has a band gap energy (3.40 eV) as semiconductors have. The band gap energy of semiconducting metal oxides (SMO) can be declined by doping strategy. among the detailed techniques like in-situ doping can be successfully applied for the decrease of band gap of materials. In the greater part of the cases the band gap of semiconductor can be modified by methods for change metal doping. There are two advantages of progress metal doping, for example, decrease of band hole, improved synergist action and surface zone. In the current examination the band gap is brought up down to 2.6 eV with the help of insitu progress metal doping (Wang et al., 2014; Rehman et al., 2017). This P-type $LaCrO_3$ exist in three different lattices depending upon the synthesis temperature, when the $LaCrO_3$ is calcined at around 830 ºC, its crystal phase is found to cubic with space group of Pm3m. The other two crystal phases of $LaCrO_3$ are hexagonal which has a space group $R^{-}3C$, while the most common crystal phase of $LaCrO_3$ nanostructure is orthorhombic phase which has a space group of Pnma (Shi et al., 2011; Thamilmaran et al., 2018).

In a significant number of the studies explored in detail, it is seen that the modified $LaCrO_3$ material is a decent dielectric material because of high polarizability. In this sense, the meaning of dielectric material can be attributed to the energy storage material as well as its usage in the catalytic applications. While perovskite materials are exceptionally productive in different applications as mentioned above, recently besides those applications the perovskite oxides are also being utilized in new different applications such as monitoring toxic gases concentration and air purification (DeCoste and Peterson, 2014). There are different procedures, like sedimentation chamber, material channel, dry and wet electro channels, ventury and rotating scrubber, activated carbons, photocatalytic oxidation (PCO), high effectiveness particulate assistance (HEPA) and so on, by which air refinement is checked (Ao and Lee, 2005; Chen et al., 2010; Ren et al., 2017; Nam et al., 2018).

The $LaCrO_3$ nanoparticles in nature have a porous structure and due to this they have very highly efficient adsorption properties. In the recent time, this material is utilized in air purification method such as controlling of concentration pollutant gases such as CO, CO_2, NO_2 etc. The fast industrialization, and auto mobilization leads to produce pollutants like NOx, CO, CO_2 etc. Many researchers are looking for suitable material, which can be used to and monitored the concentration of these pollutant emissions. The carbon dioxide is the primary gas among other greenhouse gases like CH_4, NO_2, O_3 etc. Hence its elevated concentration due to automotive exhaust and industrial discharge leads to global warming and another severe health hazards. Although the toxic effect of CO_2, this gas also being used in many applications such in production of many chemicals, fermentation in drug development, feedstock, in casting molds, soldering agent in metal industries, fire extinguisher, and in monitoring the quality of soft drinks etc. among trusted gas sensors for monitoring CO_2 the devices, there are several sensors such as non-dispersive infra-red absorption (ND-IR) and HVAC controller. One of the major drawbacks of ND-IR sensor is its large size and non-economic cost. Hence, for monitoring CO_2 and other gas concentrations most of the researchers have focused on the Chemiresistive type sensors based on metal oxide. The fabrication of Chemiresistive sensors is easy and they are low cost and thermally strong, hence the nanostructured perovskite materials are the best promising materials for sensing mechanism of the device (Fan et al., 2013; Meng et al., 2015; Sekhar et al., 2010).

The transition metals such as Ni^{2+}, Co^{2+} and Fe^{3+} are found to be very effective for tuning band gap, electrical, conducting, improving surface area, tuning crystal morphology of host lattice etc. According to several reports the, transition metal can change the host lattice taking place in the structural and crystalline properties of prepared material. According to several reports the, doping of group first and transition metals leads to enhanced metal ionic charge efficiency. In addition, the homologous elements Fe, Co, Ni are the promising metals to improve the photoreactivity and quantum yield, photoantioxidents and photoconversion of some organic compounds by several metal oxides. In many cases, it has been investigated how the transition metal doping plays a vital effective role on the properties such as dielectric, magnetic, electrical, impedance, spectroscopic properties (Herz, 2016; Adole et al., 2019; Koli et al., 2018; Pradhan and Roy, 2013; San et al., 2014; Shinde et al., 2020; Walsh, 2015). The normal oxides can be transformed to better catalyst oxides, by ease of surface doping. But in most of the cases, transition metals from 3d-5d series are the best option due to their stability in various oxidation states, good surface, high thermal stability. This surface modification leads to enhance the better electrical, conducting and surface characteristics of the particular material. Hence transition metals such as Fe, Ni, Co, Cu, V, Cr etc. are utilized for doping purpose by researchers in most of catalytical applications (Matussin et al., 2020; Xu et al., 2014; Yadav et al., 2018).

In this paper we, are revealing the transition metal doped perovskite lanthanum chromium oxide (PLCO) for the sensing of a few industrial and ozone depleting substances (greenhouse gases). In spite of the fact that an impressive work on sensors has been accounted for PLCO sensor, but in this paper, we are reporting a sensor component for CO and CO_2 gases called as greenhouse gases emitted from automobiles regularly. Increasing pollution affects nature negatively in many ways. Here we have led gas detecting work for the substances depleting ozone layer, for example, CO, CO_2, NO_2 and so forth. Our purpose in this study is to research much more focusing on CO, and CO_2 gases, besides the other ones, by means of modified $LaCrO_3$ sensors. However, we are successful to obtain some significant inferences on the sensing mechanism of these two gases. Notwithstanding, we are also revealing the likewise sensing reports for the NO_2, LPG, toluene fumes and petroleum vapours. All these gases produced from the majority of the chemical industries, metallurgical cycles, car fumes, residential processes and the centralization of these gases must be defined, hence risks due to them can be forestalled within the time Previously H_2S, NOx, Acetone gases were distinguished by utilizing perovskite sensors, however CO, CO_2, and LPG, toluene fumes and petroleum fumes are seldom announced by analysts utilizing modified $LaCrO_3$ sensors.

Thus, in the overall study of gas sensing for modified $LaCrO_3$ we were interested on sensing ability of this material for CO and CO_2 detection at various concentration of these gases. Additionally, the modified $LaCrO_3$ sensor was also utilized for humidity sensing mechanism. The impor-

tant parameters of a gas sensor such as sensitivity, selectivity, response recovery, and reusability are performed in detail for the selected gases. The results obtained for overall sensing mechanism for modified $LaCrO_3$ sensor are noteworthy and definitely promising in the field of sensors and transducers.

2. Materials and methods

All the chemicals used in the synthesis of $LaCrO_3$ nanoparticles were analytical grade and used without further purification. The chemicals like lanthanum nitrate, nickel nitrate, ferric nitrate, cobalt nitrate, chromium nitrate and citric acid were purchased from modern chemicals Nashik.

2.1. Synthesis of modified $LaCrO_3$ thin films

The crystalline, $LaCrO_3$ material modified by transition metals such as cobalt, nickel and iron was prepared by sol-gel method. In this method lanthanum nitrate hexahydrate (0.07 mol), chromium nitrate nonahydrate (0.01 mol) and citric acid (0.08 mol), were dissolved in a beaker 70 ml of double distilled water. Ni^{2+}, Fe^{3+}, and Co^{2+} salts of 5% concentration (atomic weight%) were dissolved in three separate different beakers 50 ml of double distilled water. The dopant metal nitrate concentration (5% Ni^{2+}, Fe^{3+}, $Co^{2+)}$ was added slowly to the above solution of lanthanum and chromium nitrate solution. This solution was put on a magnetic mixer and it was started to be stirred with a constant stirring speed for 30 min and 0.01 mole concentration of citric acid solution was added into this solution whose temperature was kept at 80 ˚C throughout this stirring time. After this process, color of the solution turns to the dark black-green, at this stage heating was stopped and reaction mixture was allowed to cool. This viscous black-green colored gel was used for thin films preparation. This gel was then applied on previously weighed glass substrate (1cmx2 cm) by Spin coating device with 3000 rpm and coating of the film was completed nearly 130 seconds' time. Then the obtained light green-colored thin films were dried under IR lamp for 30 min and then kept in muffle furnace for 4 h at 450 ˚C (Hussain et al., 2019; Zarrin et al., 2019).

2.2. Synthesis of undoped $LaCrO_3$ thin films

For the fabrication of undoped $LaCrO_3$ thin films, the same ways above were followed step by step. But with a difference, in this process the dopant concentration of the metals was not added during the preparation of undoped $LaCrO_3$ thin films.

2.3. Thickness measurement of the undoped and modified $LaCrO_3$ thin films

The thickness of the films was calculated by the help of the Eq. (1).

The calculated thickness of the undoped $LaCrO_3$ films was 5.128 μm and 5.41 μm for modified $LaCrO_3$. The thickness of the film was found in the thin region (Lopes et al., 2016).

$$t = \Delta M/A \times \rho \quad (1)$$

ΔM = Mass difference of the film before and after deposition.
ρ = Composite density of undoped and modified lanthanum chromium oxide ($LaCrO_3$)
A= Area of the films (Breadth = 2 cm, Height = 1.5 cm)

2.4. Characterization techniques

The XRD pattern of undoped and modified Perovskite Lanthanum chromium oxide (PLCO) was recorded by using D8 Bruker AXS GmbH (Germany), Braggs scanning angle varying from 10–80^0. The surface morphology and characteristics of the material were analysed by using scanning electron microscope (SEM), model number S 4800 Type II High Technologies Corporation, Japan. The crystal morphology was investigated by use of high-resolution transmission electron microscopy (HR-TEM) model number Jeol/JEM-2100. While the elemental composition of the thin films of modified $LaCrO_3$ was examined by using energy dispersive x-ray analysis (EDAX) spectrometer model number X-Flash detector 5030, make Bruker AXS, GmbH, Germany. The optical properties were investigated with aid of ultraviolet differential reflectance spectroscopy (UV-DRS) equipment model UV Vis NIR Spectrophotometer, Agilent Cary 200 nm to 3000 nm. The electrical properties of the thin films of modified $LaCrO_3$ were determined by using block diagram as mentioned in Fig. 8. The digital temperature controller was used to control and measure the temperature of the thin films, model number PEW-202/PEW-205. The resistance across the films was measured by using output voltage digital multimeter model number CIE classic 5175.The thin films of modified $LaCrO_3$ material were prepared by using spin coater model Delta spin RC-2100, 3000 rpm.

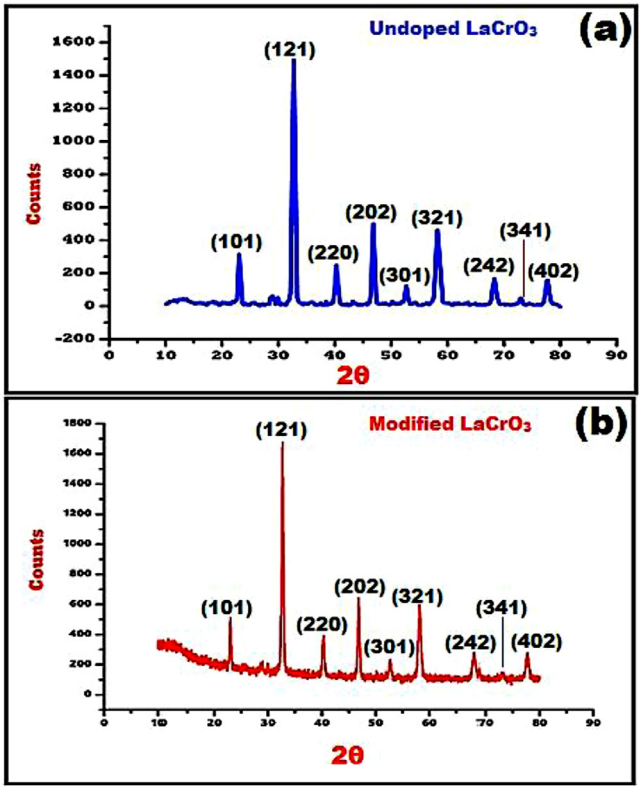

Fig. 1. (a) XRD patterns of undoped $LaCrO_3$ nanoparticles (b) XRD patterns Ni^{2+}, Fe^{3+}, Co^{2+} modified $LaCrO_3$ nanoparticles.

3. Results and discussion

3.1. X-Ray diffraction study

The XRD patterns of Ni^{2+}, Fe^{3+}, Co^{2+} incorporated Perovskite $LaCrO_3$ material and undoped $LaCrO_3$ are shown in Fig. 1a,b from which formation of crystalline $LaCrO_3$ was confirmed. These both materials were analysed by using X-ray diffraction technique with D8 Bruker AXS GmbH (Germany), Braggs scanning angle varying from 10–90˚. The MoKα radiations (wavelength1.54A^0) are used to generate the X-ray source. In the XRD spectrum as depicted in Fig. 1 from which the Bragg's reflection peaks can be assigned to the formation of crystalline $LaCrO_3$ with orthorhombic crystal lattice. The PLCO material is exist in three crystal structures such as cubic, hexagonal and orthorhombic phase. According to literature formation of $LaCrO_3$ lattice is depends on the calcination temperature. In the present research PLCO material cal-

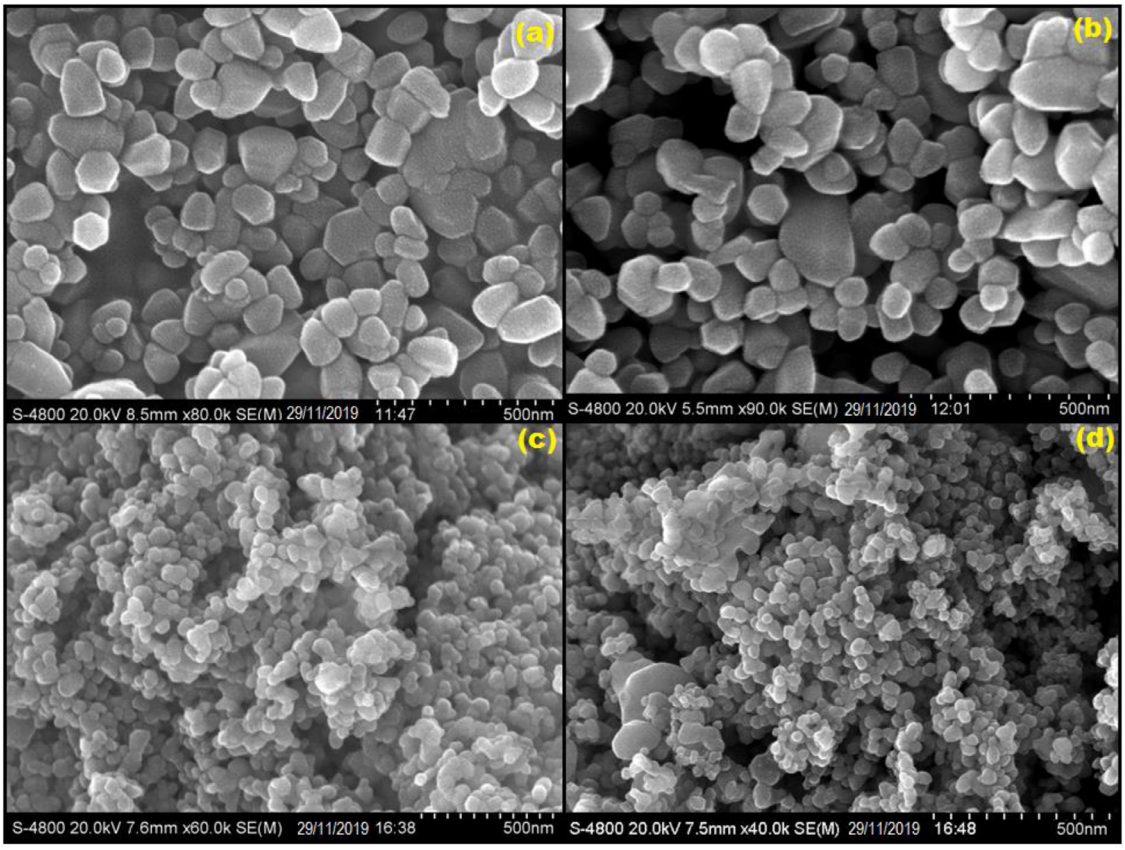

Fig. 2. (a,b) FE-SEM Images of undoped $LaCrO_3$ nanoparticles (c,d) FE-SEM Images Ni^{2+}, Fe^{3+}, Co^{2+} modified $LaCrO_3$ nanoparticles.

cined at 450 °C is formed with orthorhombic crystal lattice as depicted in Fig. 1 and confirmed from TEM data. The 2θ values of diffraction peaks obtained from XRD data for modified $LaCrO_3$ material are 23.00, 32.69, 40.26, 46.83, 52.68, 58.18, 68.33 and 77.71 The two theta values can be assigning to the reflection of (101), (121), (220), (202), (301), (321), (242), (341) and (402) planes. The diffraction peaks mentioned above confirms the formation of orthorhombic $LaCrO_3$ material. The average particle size was calculated by using Debye- Scherer's formula represented in Eq. (2).

$$D = K\lambda/\beta COS\theta \quad (2)$$

Where D is average particle size, K is constant (0.9 to 1), β is full width half maxima (FWHM) of diffracted peak, θ is the angle of diffraction. The average particle size for Ni^{2+}, Fe^{2+}, Co^{2+} modified $LaCrO_3$ was found to be 21.92 nm, while for undoped $LaCrO_3$ average particle size was 28.78 nm. The match scan data of modified $LaCrO_3$ shows the formation of crystalline $LaCrO_3$ nanoparticles with JCPDS cart number 33–0701 (Khetre et al., 2013; Zarrin et al., 2020). With doping concentration of elements probably imparts many lattice changes in host molecule like crystal defects, oxygen vacancies, F-centres, edge dislocations etc. due to this shifting of two theta values and changes in intensity may be observed in doped host lattice. Here, the line shifting or shift in two theta values is not observed may be due to minuscule doping concentration of elements.

3.2. Scanning electron microscopy (SEM)

The microstructural graphs of undoped and modified $LaCrO_3$ materials calcined at 450 °C is as shown in Fig. 2 where the nanoparticles of different size of undoped and modified $LaCrO_3$ can be observed. The lanthanum chromium oxide lattice exhibits different phases of $LaCrO_3$ material reported by the researchers. From the SEM images one can find that $LaCrO_3$ crystals are very closely agglomerated and appeared as lumps of tiny nanoparticles disperse. Between these smaller lumps the empty dark spots are appearing in the SEM images which are very small voids/smaller cavities, these voids are very helpful for the adsorption phenomenon of gas sensing (Chadli et al., 2016). Because of these cavities the smaller gases molecules may be occludedas adsorbates molecules. Most of the study on gas sensing for perovskite materials reported that adsorption of gas molecules on the surface of material as well as in the small cavities through physisorption and chemisorption mechanism on the film surface which acts as adsorbent. Since gas sensing and humidity sensing are surface entities hence surface area evaluation is an important investigation for prepared sensors. From, the SEM images material is found to porous with voids and cavities hence the available surface area calculated using BET isotherm found to be excellent for both prepared sensors. Reported SEM images found to be in good agreement with the BET isotherm study. The surface area of prepared sensors is as reported in Table 1.

3.3. High-resolution transmission electron microscopy (HR-TEM)

The crystal morphology of prepared undoped $LaCrO_3$ and Ni^{2+}, Fe^{3+}, Co^{2+} doped $LaCrO_3$ nanoparticles was observed by means of high-resolution transmission election microscopy (HR-TEM), the images of prepared materials reported in Fig. 3a–d. According to the results obtained in this study, both of these two materials have orthorhombic lattice structure, this is clearly observed from the TEM images. different estimated size of the crystallites varying from 20 to100 nm can be seen from mapping picture of HR-TEM. In Fig. 3a–d the perfect circular, oval formed nanoparticles close the orthorhombic appearance of some precious stone cross section can be seen from TEM pictures of

Table 1
BET surface area, pore volume and pore diameter of undoped $LaCrO_3$ and Ni^{2+}, Fe^{2+}, Co^{2+} modified $LaCrO_3$ nanoparticles.

Prepared Material	Surface Area (m^2/g)	Pore volume (cc/g)	Pore radius (Å)	R^2
Undoped $LaCrO_3$ films	65.34	0.350	77.40	0.9998
Ni^{2+}, Fe^{3+}, Co^{2+}modified $LaCrO_3$ films	86.32	0.396	77.77	0.9999

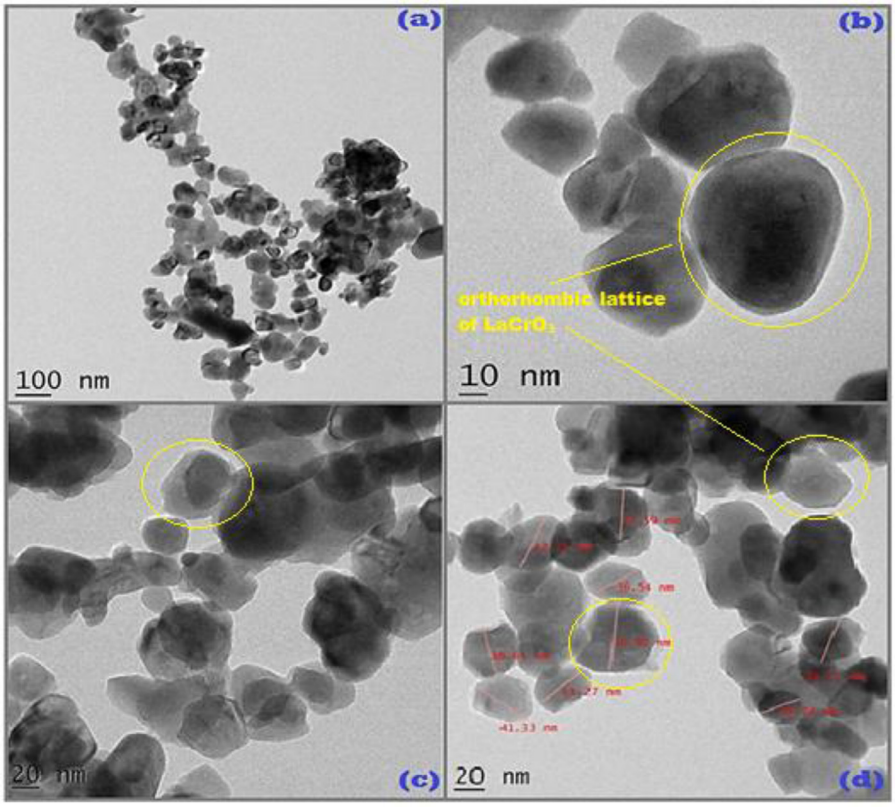

Fig. 3. (a,b) HR-TEM Images of undoped $LaCrO_3$ nanoparticles (c, d) HR-TEM Images Ni^{2+}, Fe^{3+}, Co^{2+} modified $LaCrO_3$ nanoparticles.

undoped $LaCrO_3$ and Ni^{2+}, Fe^{3+}, Co^{2+} modified $LaCrO_3$ nanoparticles. The present TEM results of undoped $LaCrO_3$ and Ni^{2+}, Fe^{3+}, Co^{2+} doped $LaCrO_3$ nanoparticles are in good concurrence with XRD and previous reported results (Shinde et.al 2020; Shinde et al., 2019).

3.4. Energy dispersive X-Ray spectroscopy (EDAX)

The EDAX spectrum of undoped $LaCrO_3$ and modified $LaCrO_3$ nanoparticles is as shown in Figure-4 from which the elemental composition of prepared undoped and modified $LaCrO_3$ sensor material is can be seen.

The sharp signals of all the elements Fe, Co, Ni, La, Cr and oxygen are observed between 4.5 to 7.5 KeV shown in EDS spectrum. The characteristic peak of lanthanum is resulted sharp at 4.5 KeV. Whereas elemental chromium is resolved at 5.5 KeV on EDS scale of both undoped and modified $LaCrO_3$. The characteristic signal of oxygen is can be seen sharp at 0.5 KeV. While the dopant metal Fe, Ni and cobalt are resoluted between 6.5 KeV to 7.5 KeV in EDS spectrum of doped $LaCrO_3$ material. The atomic weight percentage of both the prepared material viz. undoped $LaCrO_3$ and transition metal modified $LaCrO_3$ is as represented in Fig. 4a,b in tabulated form (Bagheri et al., 2018; Polat et al., 2018).

3.5. Optical properties and band gap measurements

The optical properties and band gap measurements of undoped $LaCrO_3$ and Fe^{3+}, Co^{2+} Ni^{2+}, modified $LaCrO_3$ thin films was measured by ultraviolet differential reflectance spectroscopy (UV-DRS) technique. The absorption peak and band gap are reported in Fig. 5a,b for undoped and modified $LaCrO_3$ respectively. Fig. 5a represents the absorption peak and band gap of undoped $LaCrO_3$ in which the absorption peak is reported at 334 nm from which the calculated band gap via Tauc plot is found to be Eg = 3.38 eV which is in agreement with the reported band gap undoped $LaCrO_3$. While the distance between Valence band and conduction band (band gap) for Fe^{3+}, Co^{2+}, Ni^{2+} modified $LaCrO_3$ material is found to be declined due to doping of transition metals (Naseem et al., 2014) In case of modified $LaCrO_3$ sensor the band gap energy is found to be Eg = 2.61 eV with the reduced absorption maxima 292 nm towards blue shift indicating the enhanced energy. The band gap for both these materials was calculated from following Eq. (3) (for $n = 1/2$).

$$[h\nu\alpha]^2 = (h\nu\alpha - Eg) \quad (3)$$

Where, α is the absorption coefficient, A is a constant and $h\nu$ is the photon energy

3.6. Brunauer–Emmett–Teller (BET) study

The Brunauer-Emmett-Teller (BET) study for surface area investigation was carried out for undoped $LaCrO_3$ and Fe^{3+}, Co^{2+} Ni^{2+}, modified $LaCrO_3$ material with N_2 adsorption-desorption experiment. Since, gas sensing study is a surface phenomenon between adsorbate gas molecules and adsorbent sensor material over the surface in presence of available oxygen molecules. Hence, the BET study was carried out to scrutinize

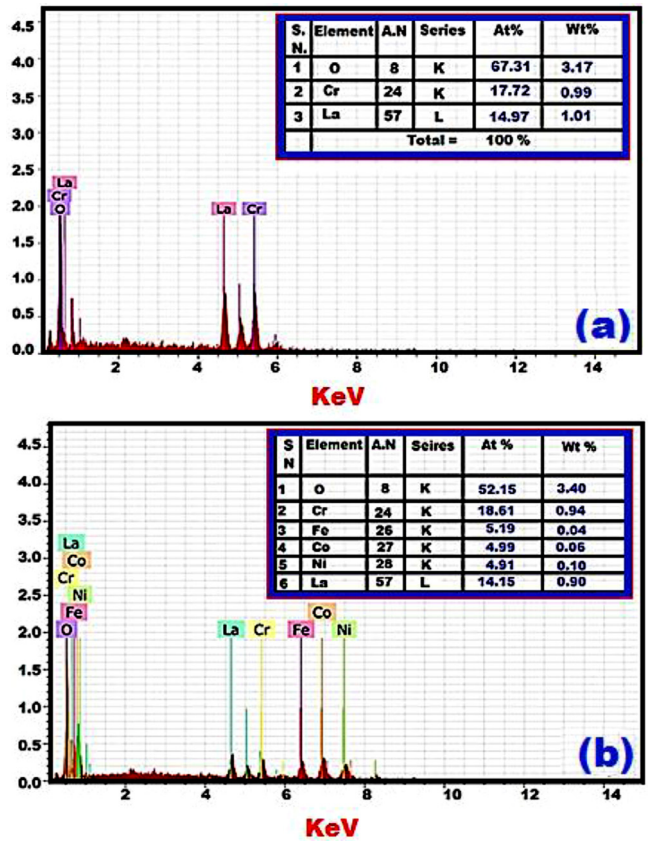

Fig. 4. (a) EDS Spectrum of undoped $LaCrO_3$ nanoparticles (b) EDS Spectrum Ni^{2+}, Fe^{3+}, Co^{2+} modified $LaCrO_3$ nanoparticles.

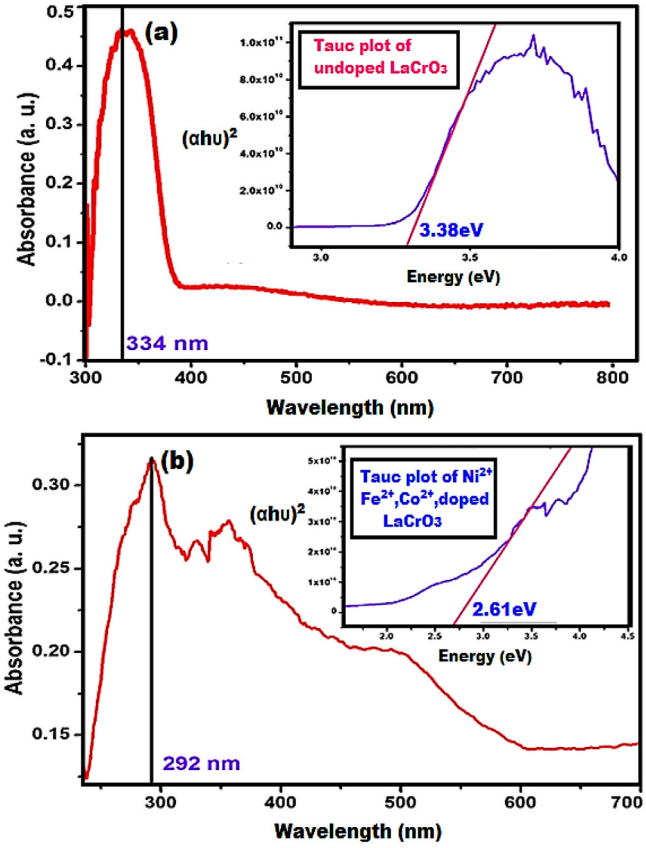

Fig. 5. (a) UV-DRS and optical band gap Spectrum of undoped $LaCrO_3$ films (b) UV-DRS and optical band gap Spectrum Ni^{2+}, Fe^{3+}, Co^{2+} modified $LaCrO_3$ films.

the surface area towards sensor material regarding porous nature, pore volume and pore radius of both prepared sensors. From BET calculations the basic surface characteristics of both prepared sensors represented in Table 1. While N_2 adsorption-desorption curves for both sensors plotted as relative pressure versus volume of the nitrogen gas and BJH pore distribution is as represented in Fig. 6. From the present investigation of BET study, it can be concluded that out of six isotherm adsorption categories according to BDDT system, the adsorption curves as mentioned in Fig. 6a,b belongs to type IV of BDDT categories of adsorption isotherm, which constitutes a distinctive porous material (Zhao et al., 2013). The surface area calculated from BET(S_{BET}), pore diameter (Dp), pore volume (Vp), correlation coefficient (R^2) parameters are exhibited in Table 1.

3.7. Electrical properties of undoped and doped Perovskite $LaCrO_3$ thin films

The solid nano materials are extensively utilized as gas sensors. The phenomenon of gas adsorption on the metal oxide surface is depends on the conducting properties of the base material. For this purpose, the metal oxide surface subjected for the electrical properties. Usually, the metal oxides show a typical semiconducting behaviour which can be easily confirmed by mounting the film for resistance calculation against a selected range of temperature. A typical semiconducting curve can be observed when the particular material shows a steady decrease in resistivity with the increase in temperature across the film surface. The reduction in resistivity of the semiconducting material is attributed to the enhancement of thermally energise flow of charge carriers which can be explained in terms of hopping control mechanism. In the simpler justification the increase temperature leads to scattering of electron hopping which is in turn decreasing the resistance of the material.

The typical semiconducting behaviour of undoped and modified $LaCrO_3$ is as shown in Fig. 7a–c and plot of Log R against 1/T for determining the activation energy of undoped and Ni^{2+}, Fe^{2+}, Co^{2+} modified $LaCrO_3$ film sensor as represented in Fig. 7b–d. Since the activation energy and resistivity are the important electronic properties and their magnitude plays vital role in chemical reactivity. Table 2 shows the resistivity of undoped $LaCrO_3$ and modified $LaCrO_3$ calculated from Eq. (4). In case of Ni^{2+}, Fe^{2+}, Co^{2+} modified $LaCrO_3$ film sensor droped value resistivity is due to the addition of dopant metal such as Ni^{2+}, Fe^{2+}, Co^{2+}. Due to doping of this metal the rate of conductivity is found to be enhanced while the resistivity is found to be slowed down. The reverse trend is observed in case of undoped $LaCrO_3$ here the resistivity value is more and conductivity value is declined. The activation energy of the sensors was calculated from Eq. (5).

$$\rho = R.b.t/L \tag{4}$$

ρ = Resistivity of the film, R = resistance at room temperature, b = breadth of film, t = thickness of the film, L = length of the film

$$R = R_0 e^{-\Delta E/KT} \tag{5}$$

R = Resistance varied at different temperatures, R_0 = Resistance at 0 °C, $\Delta E/T$ = Variation of energy with temperature i.e., activation energy, $\Delta E = 2.303 * K * Slope$ (Calculated from graph), K= Boltzmann constant (8.61733×10^{-5} eV. K^{-1})

3.8. Activation energy and transient response

The actuation vitality in the low temperature area is in every case not exactly the vitality in the high temperature region since material goes from one conduction system to another. In the low temperature region,

Table 2
Resistivity and activation energy for undoped and modified $LaCrO_3$.

Prepared Sensor	Grain Size (nm)	Resistivity (Ω m)	Activation Energy (eV)	
			L.T.	H.T.
Undoped $LaCrO_3$	21.92 nm	13.527×10^5	0.1564	0.3717
Ni^{2+}, Fe^{3+}, Co^{2+}modified $LaCrO_3$	28.78 nm	5.368×10^3	ΔE = 0.2142 eV	ΔE = 0.9979eV

(L.T. = Lower temperature, H.T. = High Temperature).

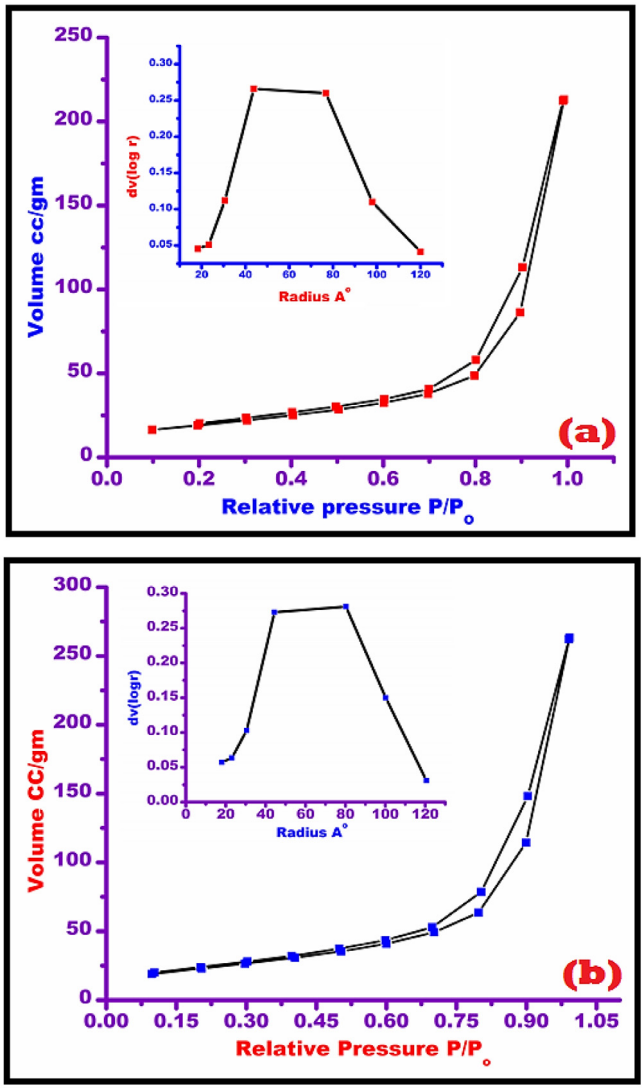

Fig. 6. BET N_2 adsorption-desorption curves for (a) undoped $LaCrO_3$ b) Ni^{2+}, Fe^{3+}, Co^{2+} modified $LaCrO_3$ thin films.

the expansion in conductivity is expected to the versatility of charge transporter, which is relying upon the imperfection, flaw or obstruction in materials. So, the conduction system is typically called the area of low temperature conduction. In this area actuation vitality diminishes since a little warm energy very adequate for the initiation of charge bearers to participate in the conduction process (Singh et al., 2019; Silva et al., al.,2016).

In alternate words the various defects, void, nullity is feebly appended in the grid can without much of a stretch move. Henceforth, increment in conductivity in the lower temperature area can be ascribed to the expansion of charge portability. In high temperature region, the enactment vitality is higher than that of low temperature locale. In this belt the electrical conductivity is chiefly dictated by the characteristic imperfections and consequently is called as natural conduction. The high estimations of actuation energy in this zone might be credited to the way that the activation expected to shape the imperfections is a lot bigger than the activation required for its float. That is the reason that natural imperfections caused by the warm changes decide the electrical conductance of the films surface is just at raised temperature.

3.9. Gas sensing study of undoped and modified $LaCrO_3$ thin films

The gas sensing study was executed by means of homemade gas sensing unit as illustrated in Fig. 8. The electrical resistance of the thick films in the presence of air (Ra), as well as in the presence of gas (Rg) was measured to calculate the gas response or sensitivity (S) given by Eq. (6). The sensitivity of Ni^{2+}, Co^{2+}, Fe^{2+} modified $LaCrO_3$ films was examined for the gases such as CO, CO_2, LPG, NO_2, Toluene vapours and petrol vapours. The sensitivity (gas response) of these gases is represented in Fig. 9a,b. According to reports $LaCrO_3$ is good sensor for H_2S, ethanol, but very few reports are reported for LPG, Petrol vapours, and greenhouse gases like CO, CO_2. As all these gas vapours are poisonous and their little concentration is highly toxic, due to this we keep emphasis to monitor these gases using undoped $LaCrO_3$ and modified $LaCrO_3$. The resistance of the prepared films was computed significantly crossed over technique. Here, modifying resistance of the thin film sensor brought about change in voltage over definite resistance. The voltage over definite resistance, i.e., particular resistance of the film is interconvertible and can be determined effectively with the guide of Ohms law. The ideal convergence of gas was presented inside the gas chamber and fixed DC voltage was applied to the film circuit. The film sensor resistance was checked by computerized yield voltage multimeter with model number CIE Classic 5170. Every time chosen gas permitted to present inside the glass chamber, the yield voltage reaction between sensor circuit and gas was recorded with multimeter. Gas residue was cleaned by supplying fixed temperature inside the gas detecting get together through thermostat.

$$S\% = Ra - Rg/Ra.100 \quad (6)$$

Ra= Resistance in presence of air, Rg= Resistance in presence of gas

The prepared sensors undoped $LaCrO_3$ and modified $LaCrO_3$ were used to sense toxic gas vapours like CO, CO_2, NO_2, LPG, toluene vapours and petrol vapours. Out of these above listed gases very rare data reported on gas sensing properties of LPG, petrol vapours (PV) and toluene vapours (TV) gases using modified $LaCrO_3$ sensor. From the collected data of gas response of all the tested gases, exhibits that these both sensors undoped $LaCrO_3$ and modified $LaCrO_3$ shows best preeminent response for CO_2 gas. The modified sensor shows sensitivity for CO_2 (82.14%) gas at 300 °C and gas concentration 1000 ppm. While for other tested gases the response recorded for modified $LaCrO_3$ showed 74.52% for CO at 200 °C, 65.18% response for NO_2 gas at 150 °C. As Well as LPG vapours showed 59.48%, toluene vapours 45.16% and petrol vapours exhibited 60.45% response at 250 °C, 350 °C and 150 °C respectively. The undoped $LaCrO_3$ also exhibited high response to CO_2 gas with 70.12% at 300 °C at gas concentration of 1000 ppm. The outstanding results for modified $LaCrO_3$ are attributed to high surface

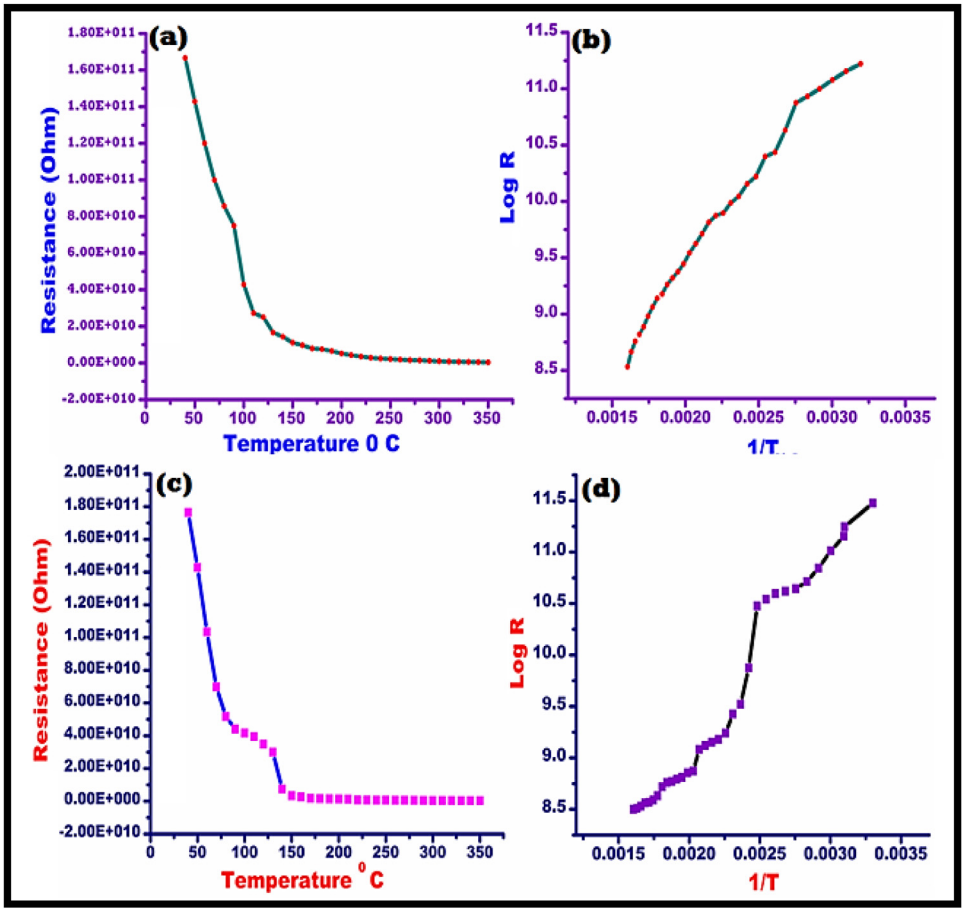

Fig. 7. (a) Variation of resistance with temperature for undoped $LaCrO_3$ film sensor (b) Plot of Log R against 1/T for activation energy of undoped $LaCrO_3$ film, (c) Variation of resistance with temperature for Ni^{2+}, Fe^{3+}, Co^{2+} modified $LaCrO_3$ film sensor (d) Plots of Log R against 1/T for activation energy of Ni^{2+}, Fe^{3+}, Co^{2+} modified $LaCrO_3$ film sensor.

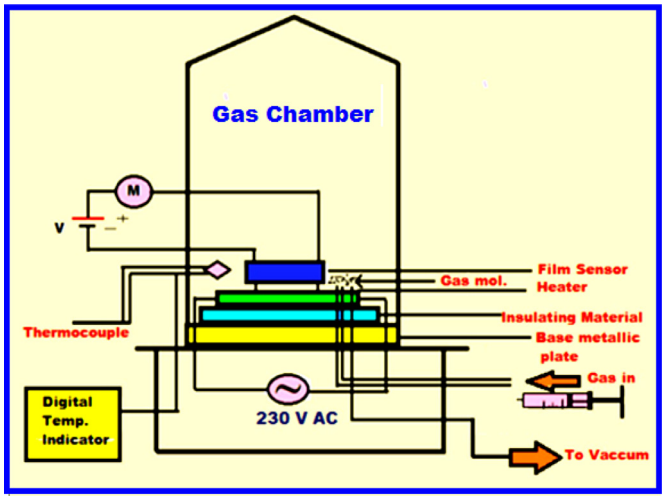

Fig. 8. Circuit diagram for gas sensing study used in present research.

area (86.32 m^2/g) from BET analysis, dwindle band gap (2.61 eV) of modified $LaCrO_3$ in comparison to undoped $LaCrO_3$. Porous nature of modified $LaCrO_3$ thin film sensor leads to highly efficient interaction between adsorbate gases and surface-active adsorbent $LaCrO_3$ sensor. Since, different gases exhibits altering energies indispensable for adsorption-desorption and chemical reactivity over the surface of semiconducting metal oxide sensor, due to this mechanism the response recorded at elevated temperature for sensor is depends upon gas to be sensed.

3.10. Selectivity and variation in gas response with gas concentration

The selectivity curves of prepared thin film sensors shown in Fig. 9c. The selectivity for tested gases was calculated using Eq. (7). In both the sensors high response recorded for CO_2. Here, each tested gas was considered to be target gas. Since the high response was recorded for carbon dioxide hence its selectivity was considered to be 100% and accordingly the selectivity was calculated as shown in Fig. 9-c. Variation in sensitivity with gas concentration of prepared thin film sensors is as shown in Fig. 9d-e. It can be observed that, gas response enhanced significantly with increase in gas concentration from 100 to 1000 ppm. The linear relationship between gas concentration and gas response may be ascribed to the accessible surface-active sensing sites over the sensor film which acted on tested gases. Lowering in gas concentration ultimately lowers the surface reaction among adsorbed oxygen molecules and adsorbate gases over film surface, which in turn gas response also decreases. On the other hand, enhancement in gas concentration leads to increase surface reaction with available oxygen molecules and this surface area coverage of gases improves gas response on the film surface.

$$\%\text{Selectivity} = \left(S_{\text{targetgas}}/S_{\text{Highrespondinggas}}\right).100 \quad (7)$$

$S_{\text{target gas}}$ – sensitivity of films for target gas
$S_{\text{High responding gas}}$- sensitivity for films for high responding gas

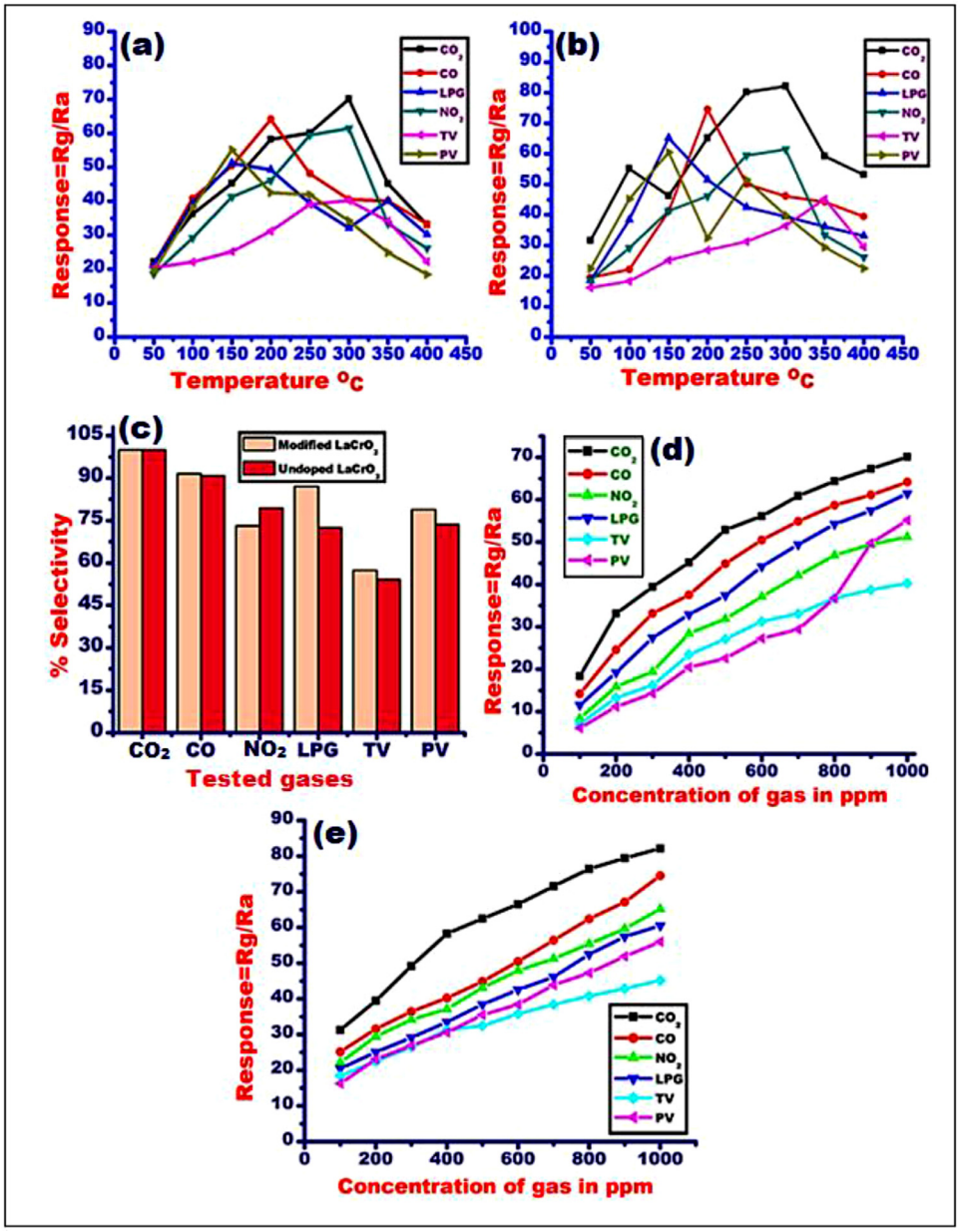

Fig. 9. (a) Gas response of tested gases at optimum temperature for undoped $LaCrO_3$ (b) Gas response of tested gases at optimum temperature for modified $LaCrO_3$ film $_{(}$c)% selectivity of undoped and modified $LaCrO_3$ film (d, e) Gas response of tested gases with change in gas concentration.

3.11. Sensing mechanism of PLCO sesnors for CO_2 gas concentration

The CO_2 is one of the major green house gas responsible for various fatal effects in human and animals. According to the reports carbon dioxide concentration at varied concentration causes different toxicological effects hazardous for animals. In medical term carbondioxide is often term as carbondioxide intoxication or dry ice poisoning. The carbon dioxide concentration was varied from 100–1000 ppm in order to get change in gas response curves, as the gas concentration changes from lower to higher concentration. The CO_2 sensing mechanism for the modified PLCO is can demonstrate as below in steps a-c.

$$O_{2\,(air)} + e\text{-} \rightarrow O_2^{-}\ (\text{adsorb}) \quad (a)$$

$$O_2 + 2e- \rightarrow 2O^{2-}\ (\text{adsorb}) \quad (b)$$

$$2CO_{2\,(gas)} + 2O^{2-}Fe^{2+}/Co^{2+}/Ni^{2+}/LaCrO_3 \rightarrow 2CO_3{}^{2-}(\text{desorb}) \quad (c)$$

The CO_2 is an oxidising gas whose interaction on the surface of modified $LaCrO_3$ film sensor is as demonstrate above in reaction a-c. The instigate CO_2 gas is desorb as a carbonate ion from the film surface. While some of the superoxide radicles ions on the sensor surface get oxidized giving rise to free electrons, get readily transferred to the conduction band of modified $LaCrO_3$. Hence, the hoping of electrons crosses the valence band of $LaCrO_3$ to outstretch the conduction band and hence the conductivity of modified $LaCrO_3$ sensor is found to be increased for CO_2 gas.

3.12. Sensing mechanism of PLCO sesnors for CO gas concentration

The exposure of CO gas vapours with nanocrystalline thin films of modified $LaCrO_3$ and its reponse at various concentratoin is represented in Fig. 9. As the sensor mechanism is a surface phenomenon, the sensors probably absorb the atmospheric oxygen on its surface and transform this oxygen into the reactive species such as peroxo (O^-), (superoxo) $O_2{}^-$ and (oxo) O^{2-} species which are very active surface entities. The interaction between $O_2{}^-$species and CO converts as $CO_3{}^-$. Adsorbed oxygen species in the form of superoxide molecules in contact with film sensor, may responsible for the redox mechanism and also gives change in output signal. Due to this a conduction of elctric field is created between oxide entities and sensor. Because of these electronic effects CO is

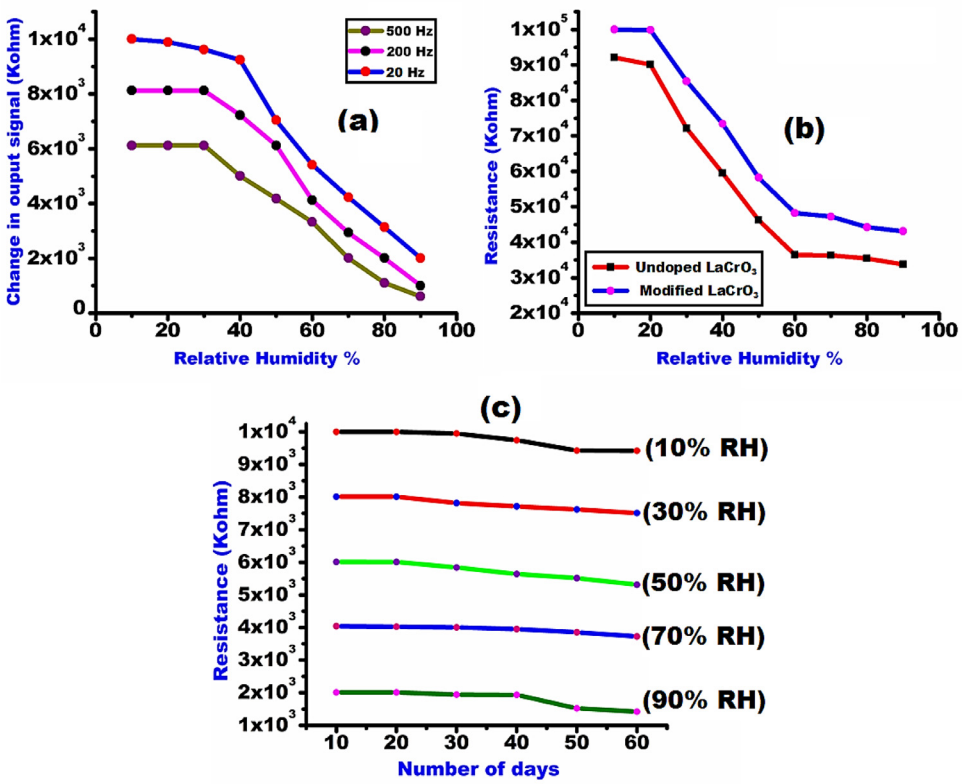

Fig. 10. (a) Dependence of output signal for relative humidity (RH) on modified $LaCrO_3$ at 20 Hz, 200 Hz, 500 Hz (b) humidity response for undoped $LaCrO_3$ and modified $LaCrO_3$ at 20 Hz (c) Stability of modified $LaCrO_3$ at various relative humidity condition for 60 days.

oxidized by charged oxide species into CO_3^- and this carbonate is evaporated from sensor surface at desired temperature, leads to improve sensing mechanism of sensor material due to desorprion of gaseous molecule from surface of sensor. Carbonate desorption from metal sensor surface can be depicted as below steps d–f. The adsorb oxide intermediates are initiated with rise in thermal conditions of the surface. These carbonates species are responsible for withdrawing the electrons from conduction band of metal oxide sensors which enhances the conductivity of metal oxide sensor. Hence, modified $LaCrO_3$ sensors are found to be very effective for the CO vapours. The mechanism of CO gas for modified $LaCrO_3$ sensor is as shown in steps d–f.

$$O_{2(air)} + e^- \rightarrow O_2^- \text{ (adsorb)} \quad \text{(d)}$$

$$O_2 + 2e^- \rightarrow 2O^{2-} \text{(adsorb)} \quad \text{(e)}$$

$$CO_{(gas)} + O_2^- \; Fe^{2+}/Co^{2+}/Ni^{2+}/LaCrO_3 \rightarrow CO_3^- \text{ (desorb)} \quad \text{(f)}$$

3.13. Sensing mechanism of PLCO for LPG gas concentration

LPG is a household gas,but at the same time it is also utilized by various industries for it's fuel applications. During the handling of these types of flammable gases the leakge detection is very necesssary and hence it is prime to detect concentration of LPG vapours by sensors. Our main interest was to investigate the concenration of LPG vapours by prepared thin film sensors. The probable constituents of LPG are methane, propane and butane in unequal concentration. From air, the dioxygen is adsorbed in the form of the species peroxo (O-), (superoxo) O_2^- and (oxo) O^{2-}. At the particular temperature these species evacuate the electron form conduction band of metal surface there by decreasing the conductivity of sensor material. The initial mechanism of LPG molecule can be started with carbon atoms that are dissociated and these dissociated molecules of carbon reacted with electrons from the conduction band of sensor material. This mechanism is accompanied with the change in the electrical properties of transition metal oxide-based sensor. The proposed reaction pathway for the LPG is can be demonstrated as below steps g-j.

$$C_4H_{10} + 13\,O^- \rightarrow 4CO_2 + 5H_2O + 13\,e^- \quad \text{(g)}$$
Butane peroxides

$$C_4H_{10} + 13O^{2-} \rightarrow 4CO_2 + 5H_2O + 13\,e^- \quad \text{(h)}$$
Butane oxides

$$C_3H_8 + 10\,O^- \rightarrow 3CO_2 + 4H_2O + 10\,e^- \quad \text{(i)}$$
Propane peroxides

$$C_3H_8 + 10\,O^{2-} \rightarrow 3CO_2 + 4H_2O + 20\,e^- \quad \text{(j)}$$
Propane oxides

From above cited steps (g-i), it can be observed that sufficient number of electrons are releasing between the interactions of oxides and superoxide with LPG on the sensor surface, leads to increase the conductivity. The researchers reported that undoped $LaCrO_3$ has less sensitivity towards LPG. Here, the dopant metals like iron, cobalt, and nickel are expected as promoters to dissociate the oxygen over the $LaCrO_3$ surface which is in turn enhance the sensitivity of LPG towards the modified $LaCrO_3$ sensor.

3.14. Humidity sensing performance of undoped and modified $LaCrO_3$ thin films sensor

The relative humidity (RH) is one of the prime parameters for a sensing device, associated to real vapour pressure of water to the saturated vapour pressure of water at the specific temperature. In common humidity sensors the altering electric output signal with the change in humidity arised from adsorption of water molecule over the surface of sensor. Here both the sensors undoped $LaCrO_3$ and modified $LaCrO_3$ utilised for humidity sensing mechanism. The change in electric output signal versus relative humidity resoluted at various frequencies is as shown in Fig. 10-a. It can be seen from figure –10, that the change in electric output signal is emphatically overblown by operating frequency range, at lower frequency range the output signal is found to be most af-

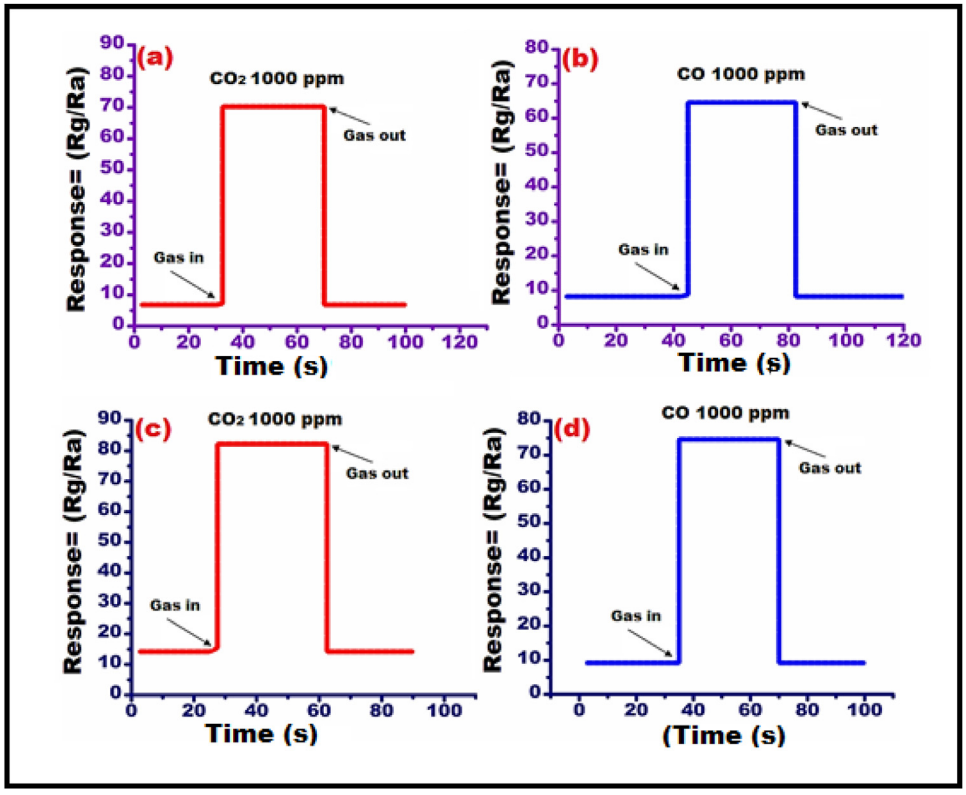

Fig. 11. (a, b) Response and recovery curves for CO_2, CO gases atundoped $LaCrO_3$ sensor (c, d) Response and recovery curves for CO_2, CO gases atmodified$LaCrO_3$ sensor.

fected. When the relative humidity is varied from 10% to 90% at 20 Hz, the change in electric output signal found to be declined continuously and shown the highest humidity sensing response at this frequency i.e. 20 Hz. Hence the 20 Hz frequency operating range for humidity sensor was chosen to be fixed operating range for further studies. In overall comparison relative humidity sensing experiment, for undoped and modified $LaCrO_3$ thin film sensor, the modified $LaCrO_3$ found to be more effective for humidity sensing, the reason for this behaviour by modified $LaCrO_3$ attributed to high surface area, porous nature and smaller band gap energy. Undoped and modified $LaCrO_3$ were utilized for the humidity characteristics at 20 Hz, these curves for both materials are as depicted in Fig. 10–b. Both these sensors were utilized from low to high relative humidity, the rapid change in resistance (output signal) for undoped and modified $LaCrO_3$ is can be seen from Fig. 10-b, associated with the adsorption process. The curves show that, the change in output signal due to adsorption process at low characteristics values of relative humidity makes the modified $LaCrO_3$ an effective humidity sensor. In every humidity sensor, the probable electronic mechanism over the surface of sensor is turn on formation of proton ions (H^+) and hydronium ions (H_3O^+) due to dissociation of aqua molecules. These two species have interconnection to form hydroxyl (OH^-) ions. The percent response of every metal oxide-based sensor will be diminished with rise in aqua molecules over the film surface, the reason behind that is sensor surface not effectively contributes in redox mechanism. The most important characteristic of a sensor when it utilized as any type of sensor like humidity sensor or gas sensor is its long-time stability. The stability of modifed $LaCrO_3$ for relative humidity was observed for 60 days. From Fig. 10-c it can be seen that output signal varies very slightly with the change in various relative humidity concentrations. Thus, it can be concluded that modified $LaCrO_3$ sensor can be effectively employed as humidity sensor at elevated humidity concentration.

3.15. Response and recovery of undoped and modified $LaCrO_3$ thin films sensor for co and CO_2 gases

The undoped and modified $LaCrO_3$ sensors were utilized for sensing of CO, CO_2, NO_2, LPG, toluene vapours and petrol vapours. Out of these tested gases CO, CO_2, NO_2 and LPG gases are found be sensitive for prepared sensors. After that we switch our attention towards response and recovery properties of greenhouse gases CO and CO_2. For rapid detection of these gases, the response and recovery set were explored. The response and recovery curves of CO and CO_2 gases for undoped and modified $LaCrO_3$ depicted in Fig. 11a-d. Initially the undoped $LaCrO_3$ sensor was utilized for response and recovery properties. For carbon dioxide gas, the response time was 30 s. While recovery time of undoped $LaCrO_3$ sensor for CO_2 gas was 70 s at 1000 ppm gas concentration. At the same time CO gas response time for undoped $LaCrO_3$ was 45 s and recovery time was 83 s. Modified $LaCrO_3$ sensor was utilized for the same gases CO and CO_2 to get the comparative results. The CO_2 gas response time for modified $LaCrO_3$ sensor found to be 28 s and fast recovery time was recorded for modified sensor. The CO gas response at 1000 ppm concentration for Fe^{2+},Co^{2+},Ni^{2+}modified $LaCrO_3$ was 35 s and recovery were very rapid about 70 s. Therefore, in overall study the Fe^{2+},Co^{2+},Ni^{2+} modified $LaCrO_3$ found to be excellent in response and recovery study for CO and CO_2 gases. There are many rationales to discuss the improved response and recovery properties of modified sensor, probably the dopant concentration can be effective to enhance electronic and surface properties of the modifed $LaCrO_3$ sensor. The sensitivity (response) and recovery timescale for tested gases CO and CO_2 at undoped $LaCrO_3$ and modified $LaCrO_3$ is as shown in Fig. 12.

3.16. Recycling performance of prepared sensors for high responding gases CO and CO_2

For powerful working of any gas sensor, it must comply with the boundaries like fast activity of sensor, thermal stability, high response and recovery, good sensitivity for tested gases and most important is sensor reusability. To get the reproducible outcomes, the prepared modified $LaCrO_3$ sensor was utilized for recycling performance for high responding gases CO and CO_2. The ideal conditions followed for reusability was the gas concentration was kept up at 1000 ppm, the prepared film sensor, and same set up delineated in Figure –7 was used. The reusing for CO and CO_2 gases was by modified $LaCrO_3$ was led with time frame days. In the main run of 10 days the modified $LaCrO_3$ showed 74.50%

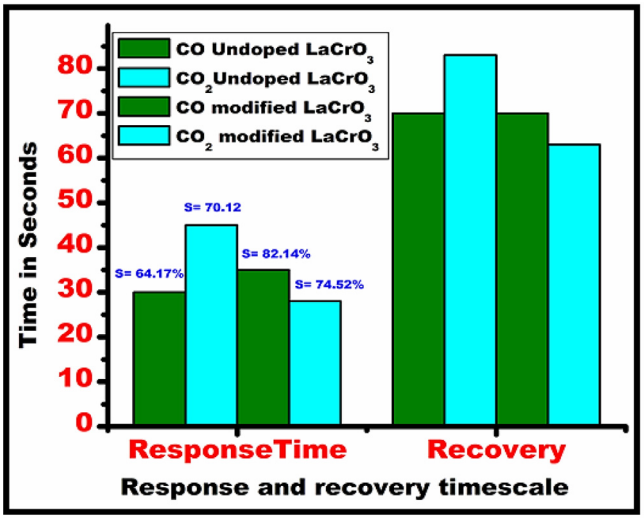

Fig. 12. Response and recovery timescale of CO and CO_2 gases for undoped and modified $LaCrO_3$ sensor.

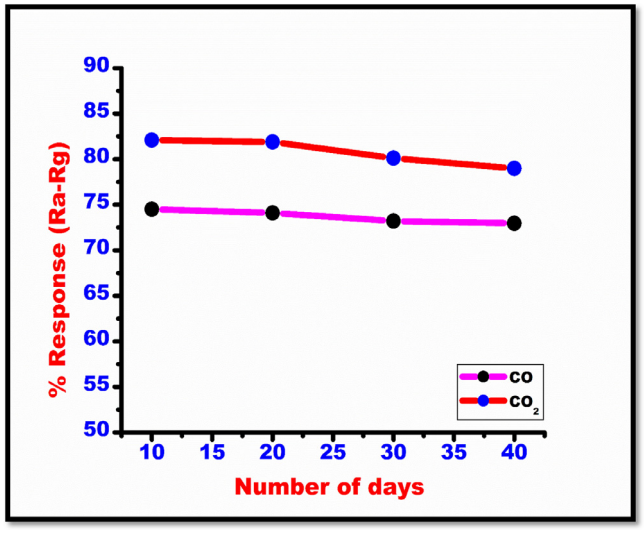

Fig. 13. Reusability performances by modified $LaCrO_3$ for CO and CO_2 gases.

for CO and 82.10% for CO_2 gas. Then after 20 days for example second run for modified $LaCrO_3$ the reaction for CO and CO_2 recorded was 74.10% and 81.90% individually. At the same time the sensor following 30 and 40 days indicated response 72.20%, 72.95% for CO and 80.12%, 79.90% response for CO_2 gas. In generally test it is seen that the precision of reusability test was about 98% and sensor discovered to be exceptionally proficient and reproducible for CO and CO_2 gases. Here the inspection about the decrease in% sensitivity for every interval of 10 days can be attributed to decrease in surface activeness of the modified $LaCrO_3$ sensor as the sensor mistreated regularly for the testing, the upper surface development found to bring down because of revealing of gas each time therefore its adsorption property cut down. Along these lines, steady decrease found in the affectability response by the sensor. The reproducibility of the modified $LaCrO_3$ sensor for CO and CO_2 gases is as delineated in Fig. 13.

3.17. Comparison of prepared sensors for CO and CO_2 gases

Gas sensors have prime importance now days, due their high-class demand at various places. Researchers have utilized various materials to prepare effective sensors to sense toxic, harmful environmental pollutants and industrial pollutant gases. As per literature survey undoped $LaCrO_3$ film sensors effectively utilized to sense the gases like H_2S, NH_3, Acetone, CH_3-OH, C_2H_5-OH, Methane, Cl_2, Br_2 and relative humidity. Even undoped $LaCrO_3$ is modified in the form of nanocomposites or binary oxides by some researchers to sense the common pollutant gases. But comparative results of undoped and transition metal doped $LaCrO_3$ are not reported. Hence, we keep emphasis to demonstrate the comparative results for these both sensors for CO and CO_2 gases. Although in comparative investigation we found that there are plenty of material sensors utilized for sensing of CO and CO_2 gases. But using perovskite $LaCrO_3$ sensor, the gases like CO and CO_2 gas sensing and humidity sensing properties are not reported in detail. Thus, in the present investigation of comparative results between modified $LaCrO_3$ and rest of the other reported sensors for CO and CO_2 gas sensing, the modified $LaCrO_3$ is quite effective, excellent and reproducible sensor.

4. Conclusions

The undoped $LaCrO_3$ and transition metals Ni^{2+}, Fe^{3+}, Co^{2+} modified $LaCrO_3$ sensor [perovskite lanthanum chromium oxide (PLCO)] was prepared by sol-gel- spin coating route. The materials synthesis is low cost, while prepared sensors found to be efficient, crystalline and porous, containing high surface area. The prepared sensors undoped and modified $LaCrO_3$ utilized to sense the gases CO, CO_2, NO_2, LPG, toluene vapours and petrol vapours. The modified $LaCrO_3$ sensor found to be highly sensitive for CO and CO_2 gases at 300 °C and 200 °C, respectively. While for other gases like NO_2, LPG, toluene vapours and petrol vapours, the modified $LaCrO_3$ is moderately sensitive. The gas sensing mechanism for CO, CO_2 and LPG gases was established successfully. In addition, the modified $LaCrO_3$ sensor was effectively employed for gas response, selectivity, the humidity sensing performance, response recovery and reusability performance. For all the listed properties the modified $LaCrO_3$ sensor was very effective in terms of sensing properties. The relative humidity experiment was performed from 10 to 90% humidity, where the highest humidity response for modified PLCO sensor was recorded at 20 Hz. From overall results, it is found that transition metals Ni^{2+}, Fe^{3+}, Co^{2+} doping was successful to modify $LaCrO_3$ lattice. Due to doping of transition metals, the properties such as band gap energy, surface area and porosity properties found to be enhanced and altered. In the overall concluding it can be suggested that modified $LaCrO_3$ sensor is highly efficient sensor for CO, CO_2, and relative humidity in comparison to the undoped $LaCrO_3$ due to enhanced porosity, declined band gap and high surface area of modified $LaCrO_3$ sensor. As per as previous research for undoped $LaCrO_3$ the detailed gas sensing properties for greenhouse gases and relative humidity was not explained. The proposed research of modified $LaCrO_3$ is very successful to encompass the important greenhouse gas sensing properties and relative humidity. Thus, modified $LaCrO_3$ gas sensor can be effectively applied as reproducible and reliable gas sensor for greenhouse gases, LPG and relative humidity.

Declaration of Competing Interest

On behalf of all the listed authors above, I Mr. Prashant Bhimrao Koli (Corresponding author) declares that, we have not received any funding for the research work and we have no conflict of interest for our research work.

Acknowledgments

Authors are gratefully acknowledged to the STIC, Cochin University, Kerala for XRD, TEM and UV-DRS results, SAIF-UDCT, Jalgaon (M.S) for SEM, EDS, and IR studies. Authors are thankful to SAIF – SPPU Pune University for BET results. Authors also extend sincere thanks to Department of chemistry, Pratap College, Amalner, Department of Chemistry, L.V.H. College, Department of electronics, L.V.H. College,

Panchavati, Nashik (MAH, India) for providing necessary laboratory facilities. Authors are also grateful to Department of Chemistry, ACS, College, Nandgaon, District- Nashik, Department of Chemistry, KVN Naik College, Nashik and Department of physics (Applied science), MITWPU, School of polytechnic, Pune.

References

Adeel, M., Rahman, M.M., Caligiuri, I., Canzonieri, V., Rizzolio, F., Daniele, S., 2020. Recent advances of electrochemical and optical enzyme-free glucose sensors operating at physiological conditions. Biosens. Bioelectron. 165, 1–13.

Adole, V.A., Pawar, T.B., Koli, P.B., Jagdale, B.S., 2019. Exploration of catalytic performance of nano-La_2O_3 as an efficient catalyst for dihydropyrimidinone/thione synthesis and gas sensing. J. Nanostructure Chem. 9, 61–76.

Bagheri, A., Javanbakht, M., Hosseinabadi, P., Beydaghi, H., Shabanikia, A., 2018. Preparation and characterization of SPEEK/SPVDF-co-HFP/$LaCrO_3$ nanocomposite blend membranes for direct methanol fuel cells. Polymer 138, 275–287.

Bataglioli, R.A., Taketa, T.B., Neto, J.R., Lopes, L.M., Costa, C.A.R., Beppu, M.M., 2019. Analysis of pH and salt concentration on structural and model-drug delivery properties of polysaccharide-based multilayered films. Thin Solid Films 685, 312–320.

Chadli, I., Omari, M., Dalo, M.A., Albiss, B.A., 2016. Preparation by sol–gel method and characterization of Zn-doped $LaCrO_3$ perovskite. J. Sol-Gel Sci. Technol. 80, 598–605.

Chen, J., Shen, M., Wang, X., Wang, J., Su, Y., Zhao, Z., 2013. Catalytic performance of NO oxidation over LaMeO3 (Me= Mn, Fe, Co) perovskite prepared by the sol–gel method.. Catal. Commun. 37, 105–108.

Ao, C.H., Lee, S.C., 2005. Indoor air purification by photocatalyst TiO_2 immobilized on an activated carbon filter installed in an air cleaner. Chem. Eng. Sci. 60, 103–109.

Chen, C.Q., Li, W., Cao, C.Y., Song, W.G., 2010. Enhanced catalytic activity of perovskite oxide nanofibers for combustion of methane in coal mine ventilation air. J. Mater. Chem. 20, 6968–6974.

DeCoste, J.B., Peterson, G.W., 2014. Metal–organic frameworks for air purification of toxic chemicals. Chem. Rev. 114, 5695–5727.

Ding, H., Xue, X., 2010. $GdBa_{0.5}Sr_{0.5}Co_2O_{5+\delta}$ layered perovskite as promising cathode for proton conducting solid oxide fuel cells. J. Alloys Compd. 496 (1–2), 683–686.

Fan, K., Qin, H., Wang, L., Ju, L., Hu, J., 2013. CO_2 gas sensors based on $La_{1-x}Sr_xFeO_3$ nanocrystalline powders. Sens. Actuators B Chem. 177, 265–269.

Herz, L.M., 2016. Charge-carrier dynamics in organic-inorganic metal halide perovskites. Ann. Rev. Phys. Chem. 67, 65–89.

Huang, S., Gao, F., Meng, Z., Feng, S., Sun, X., Li, Y., Wang, C., 2014. Bismuth-based perovskite as a high-performance cathode for intermediate-temperature solid-oxide fuel cells. Chem. Electro. Chem. 1, 554–558.

Hussain, S., Javed, M.S., Ullah, N., Shaheen, A., Aslam, N., Ashraf, I., Abbas, Y., Wang, M., Liu, G., Qiao, G., 2019. Unique hierarchical mesoporous $LaCrO_3$ perovskite oxides for highly efficient electrochemical energy storage applications. Ceram. Int. 45, 15164–15170.

Jain, G.H., Patil, L.A., Wagh, M.S., Patil, D.R., Patil, S.A., Amalnerkar, D.P., 2006. Surface modified $BaTiO_3$ thick film resistors as H_2S gas sensors. Sens. Actuators B Chem. 117, 159–165.

Jiao, W., He, J., Zhang, L., 2020. Synthesis and high ammonia gas sensitivity of $(CH_3NH_3)PbBr_{3-x}I_x$ perovskite thin film at room temperature. Sens. Actuators, B. 309, 127786.

Kim, S.M., In, I., Park, S.Y., 2016. Study of photo-induced hydrophilicity and self-cleaning property of glass surfaces immobilized with TiO_2 nanoparticles using catechol chemistry. Surf. Coat. Technol. 294, 75–82.

Khetre, S.M., Chopade, A.U., Khilare, C.J., Jadhav, H.V., Jagadale, P.N., Bamane, S.R., 2013. Electrical and dielectric properties of nanocrystalline $LaCrO_3$. J. Mater. Sci. 24, 4361–4366.

Koli, P.B., Kapadnis, K.H., Deshpande, U.G., More, B.P., Tupe, U.J., 2020. Sol-Gel fabricated transition metal Cr_3^+, Co_2^+ doped lanthanum ferric oxide (LFO-$LaFeO_3$) thin film sensors for the detection of toxic, flammable gases: a comparative study. Mater. Sci. Res. India. 17, 70–83.

Koli, P.B., Kapadnis, K.H., Deshpande, U.G., 2019. Transition metal decorated Ferrosoferric oxide (Fe_3O_4): an expeditious catalyst for photodegradation of Carbol Fuchsin in environmental remediation. J. Environ. Chem.Eng. 7, 103373.

Koli, P.B., Kapadnis, K.H., Deshpande, U.G., Patil, M.R., 2018a. Fabrication and characterization of pure and modified Co_3O_4 nanocatalyst and their application for photocatalytic degradation of eosine blue dye: a comparative study. J. Nanostruct. Chem. 8, 453–463.

Koli, P.B., Kapadnis, K.H., Deshpande, U.G., 2018b. Nanocrystalline-modified nickel ferrite films: an effective sensor for industrial and environmental gas pollutant detection. J. Nanostruct. Chem. 9, 95–110.

Lopes, F., Cardozo Amorin, L.H., da Silva Martins, L., Urbano, A., Roberto Appoloni, C., Cesareo, R., 2016. 2016 thickness measurement of V_2O_5 nanometric thin films using a portable XRF. J. Spectrosc 2016, 1–7. doi:10.1155/2016/9509043.

Matussin, S.N., Harunsani, M.H., Tan, A.L., Cho, M.H., Khan, M.M., 2020. Effect of Co_2^+ and Ni_2^+ co-doping on SnO_2 synthesized via phytogenic method for photoantioxidant studies and photoconversion of 4-nitrophenol. Mater. Today Commun. 25, 101677.

Meng, F.L., Guo, Z., Huang, X.J.;, 2015. Graphene-based hybrids for Chemiresistive gas sensors. Trac-trend anal chem 68, 37–47.

Morozova, L.V., Kalinina, M.V., Tikhonov, P.A., Drozdova, I.A., Shilova, O.A., 2017. Electroconducting ceramics based on In_2O_3, CdO, and $LaCrO_3$. Glass Phys. Chem. 43, 276–281.

Nam, H., Wang, S., Jeong, H.R., 2018. TMA and H_2S gas removals using metal loaded on rice husk activated carbon for indoor air purification. Fuel 213, 186–194.

Naseem, S., Khan, W., Saad, A.A., Shoeb, M., Ahmed, H., Husain, S., Naqvi, A.H., 2014. Variation in band gap of lanthanum chromate by transition metals doping $LaCr_{0.9}A_{0.1}O_3$ (A: fe/Co/Ni). AIP Conf. Proc 1591, 259–261.

Polat, O., Durmus, Z., Coskun, F.M., Coskun, M., Turut, A., 2018. Engineering the band gap of $LaCrO_3$ doping with transition metals (Co, Pd, and Ir). J. Mat. Sci. 53, 3544–3556.

Pradhan, S., Roy, G.S., 2013. Study the crystal structure and phase transition of $BaTiO_3$–A pervoskite. Researcher 5, 63–67.

Rehman, W., McMeekin, D.P., Patel, J.B., Milot, R.L., Johnston, M.B., Snaith, H.J., Herz, L.M., 2017. Photovoltaic mixed-cation lead mixed-halide perovskites: links between crystallinity, photo-stability and electronic properties. Energy Environ. Sci. 10, 361–369.

Ren, H., Koshy, P., Chen, W.F., Qi, S., Sorrell, C.C., 2017. Photocatalytic materials and technologies for air purification. J. Hazard. Mater. 325, 340–366.

San, Ha, Le, N., V.T., Goo, N.S., 2014. Investigation of fracture properties of a piezoelectric stack actuator using the digital image correlation technique. Int. J. Fatigue. 101, 106–111.

Sekhar, P.K., Brosha, E.L., Mukundan, R., Garzon, F., 2010. Chemical sensors for environmental monitoring and homeland security. Electrochem. Soc. Interface 19, 35.

Shi, J., Ye, J., Zhou, Z., Li, M., Guo, L., 2011. Hydrothermal synthesis of $Na_{0.5}La_{0.5}TiO_3$–$LaCrO_3$ solid-solution single-crystal nanocubes for visible-light–driven photocatalytic H_2 evolution. Chemistry–A European Journal, 17, 7858–7867.

Shinde, S.G., Patil, M.P., Kim, G.D., Shrivastava, V.S., 2020a. Ni, C, N, S multi-doped ZrO_2 decorated on multi-walled carbon nanotubes for effective solar induced degradation of anionic dye. J. Environ. Chem.Eng. 8, 103769.

Shinde, V.S., Sawant, C.P., Kapadnis, K.H., 2019. Modified Sn-doped $LaCrO_3$ nanostructures: focus on their characterization and applications as ethanol sensor at a lower temperature. J. Nanostructure. Chem. 9, 231–245.

Shinde, V.S., Kapadnis, K.H., Sawant, C.P., Koli, P.B., Patil, R.P., 2020b. Screen print fabricated in^{3+} decorated perovskite lanthanum chromium oxide ($LaCrO_3$) thick film sensors for selective detection of volatile petrol vapors. J. Inorg. Organomet. Polym. Mater. 30, 5118–5132.

Silva, R.S., Barrozo, P., Moreno, N.O., Aguiar, J.A., 2016. Structural and magnetic properties of $LaCrO_3$ half-doped with Al. Ceram. Int. 42, 14499–14504.

Singh, R.D., Koli, P.B., Jagdale, B.S., Patil, A.V., 2019. Effect of firing temperature on structural and electrical parameters of synthesized CeO_2 thick films SN Appl. Sci. 1, 315.

Slonopas, A., Ryan, H., Norris, P., 2019. Ultrahigh energy density $CH_3NH_3PbI_3$ perovskite-based supercapacitor with fast discharge. Electrochim. Acta 307, 334–340.

Tan, H., Zhao, Z., Zhu, W.B., Coker, E.N., Li, B., Zheng, M., Yu, W., Fan, H., Sun, Z., 2014. Oxygen vacancy enhanced photocatalytic activity of pervoskite $SrTiO_3$. ACS Appl. Mater. Interfaces. 6 (21), 19184–19190.

Thamilmaran, P., Arunachalam, M., Sankarrajan, S., Sakthipandi, K., Sivabharathy, M., Samuel, E.J.J., 2018. Structural transition in Gd doped $LaCrO_3$ isovalent by in-situ ultrasonic measurements. Physica B 530, 270–276.

Walsh, A., 2015. Principles of chemical bonding and band gap engineering in hybrid organic–inorganic halide perovskites. J. Phys. Chem. C. 119, 5755–5760.

Wang, F., Grinberg, I., Rappe, A.M., 2014. Band gap engineering strategy via polarization rotation in perovskite ferroelectrics. Appl. Phys. Lett. 104, 152903.

Xu, X.X., Cui, Z.P., Gao, X., Liu, X.X., 2014. Photocatalytic activity of transition-metal-ion-doped coordination polymer (CP): photoresponse region extension and quantum yields enhancement via doping of transition metal ions into the framework of CPs. Dalton Trans. 43, 8805–8813.

Yadav, R.S., Kuřitka, I., Vilcakova, J., Havlica, J., Kalina, L., Urbánek, P., Machovsky, M., Skoda, D., Masař, M., Holek, M., 2018. Sonochemical synthesis of Gd^{3+} doped $CoFe_2O_4$ spinel ferrite nanoparticles and its physical properties. Ultrason. Sonochem. 40, 773–783.

Zarrin, N., Husain, S., Gaur, D.D., Somvanshi, A., Fatema, M., 2020. Dopant incited alterations in structural, morphological, optical, and dielectric properties of Er-doped $LaCrO_3$. J. Mater. Sci.: Mater. 31, 3466–3478.

Zarrin, N., Husain, S., Khan, W., Manzoor, S., 2019. Sol-gel derived cobalt doped $LaCrO_3$: structure and physical properties. J. Alloys Compd. 784, 541–555.

Zhang, W., Eperon, G.E., Snaith, H.J., 2016. Metal halide perovskites for energy applications. Nature Energy 1, 1–8.

Zhang, C., Guo, Y., Guo, Y., Lu, G., Boreave, A., Retailleau, L., Baylet, A., Giroir-Fendler, A., 2014. $LaMnO_3$ perovskite oxides prepared by different methods for catalytic oxidation of toluene. Appl. Catal. B. 148, 490–498.

Zhang, C., Wang, Y., Chen, X., Chen, H., Wu, Y., Wang, Y., Tang, L., Cui, G., Chen, D., 2020. Catalytic behavior of $LaFeO_3$ pervoskite oxide during low-pressure gas nitriding. Appl. Surf. Sci. 506, 145045.

Zhao, J., Liu, Y., Li, X., Lu, G., You, L., Liang, X., Liu, F., Zhang, T., Du, Y., 2013. Highly sensitive humidity sensor based on high surface area mesoporous $LaFeO_3$ prepared by a nanocasting route. Sens. Actuators B. 181, 802–809.